CONCRETE LIBRARY OF JSCE NO. 29, JUNE 1997

TIME-DEPENDENT BEHAVIOUR OF CONCRETE AT AN EARLY AGE AND ITS MODELLING

(Translation from Proceedings of JSCE, No.520/V-28, August 1995)


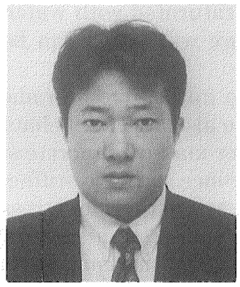

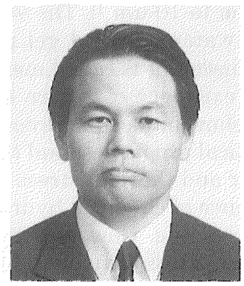

Yasuaki ISHIKAWA Hideki OHSHITA Hirotoshi ABE Tada-aki TANABE

A mathematical model of early-age concrete is presented and used to investigate its time dependent behaviour. The study concentrates on the role of pore water in creep and relaxation. Several experimental results are analyzed with the model and the effect of pore water effect on early-age concrete is discussed.

Keywords: early-age concrete, pore pressure, creep, relaxation

---

Yasuaki Ishikawa is an assistant in the Department of Civil Engineering at Meijo University, Nagoya, Japan. He obtained his M.Sc. from Nagoya University in 1993. He is a member of the JSCE

Hideki Ohshita is an Assistant Professor in the Department of Civil Engineering at the National Defense Academy, Yokosuka, Japan. He obtained his D.Eng. from Nagoya University in 1995. He is a member of the JSCE.

Hirotoshi Abe belonged to the Central Research Institute of Electric Power Industry. He obtained his B.Eng. from Tohoku University in 1957. He is a member of the JSCE.

Tada-aki Tanabe is a Professor in the Department of Civil Engineering at Nagoya University. He obtained his D.Eng. from the University of Tokyo in 1971. He is a member of the JSCE.

1. INTRODUCTION

Concrete properties change rapidly in the few days following the mixing of water into the cement. Hydration is induced at the interface between pore water and particles of cement. CSH gels form. This results in voids with diameters of a few decades of Å. The initial distribution of void diameter is determined by the distribution of cement particles as well as the distribution of aggregates in the mixture. The initial size of cement particles is almost the same as the initial minimum pore size which is almost 1 um. Next, CSH gel penetrates into voids and forms smaller voids. CSH gel is said to have a size of $10 \sim 10^4$Å near unhydrated cement particles separated by voids and aggregates with sizes from 10^2um to 10^5um [1]. The void system is thought to be saturated with water, especially in the beginning. The water is called gel pore water or cappillary pore water and can be vaporized. In the following discussion, it is called merely pore water.

The existence of a pore system naturally affects the initial stress gradient if pore water pressure is somehow induced. Moreover, the initial concrete state also affects behaviour at a later age in terms of physical properties, and this is especially important for massive concrete structures; hydration heat can occur and thermal stress problems may be induced. Since concrete stiffness may be increased with the advance of chemical hydration at an early age, compressive thermal stresses may be mainly induced in the concrete. However, in the few days after casting, the stress history reveals a contrary pattern and tensile stress may be induced. At this stage, creep deformation may govern and may offset the stress. However, these effect have not been clarified. If a deformational analysis of the creep problem is performed, the creep function for hardened concrete may be interpolated. If the pore water has an effect, however, it is the effect of size dependent. It is said that concrete creep is generally larger if a member size is smaller. However, creep is a material property and does not depend on size, while pore water migration is a process of diffusion. Moreover, the effect of creep of compression and tension is considered to be the same, while the effect of pore water in the compressive stress state is quite different to that in tension. The time dependent behaviour of concrete at an early age can be assumed to be affected by pore water in the concrete, although a clear mechanism is still being investigated.

Conventional research with respect to the migration of pore water in concrete began Lynam[2] who applied the seepage theorem to concrete creep. Later, many researchers including Powers[3] and Bazant[4] discussed the permeability of concrete both experimentally and theoretically. Neville[5] has also reported that concrete creep under a sustained load is mainly affected by the migration of pore water. However, much of this research has been performed experimental, so the mechanism of time-dependent behaviour due to pore water has not been sufficiently clarified theoretically. A mathematical model that predicts these phenomena with considerable accuracy is demanded.

In this paper, early-age concrete is modeled as a two-phase porous material consisting of aggregate and cement paste plus pore water, and the effects of migration of pore water at an early age are investigated.

2. MODELLING OF EARLY-AGE CONCRETE AS A TWO-PHASE SATURATED POROUS MATERIAL

Particles of CSH gel and aggregate can be considered as elastic bodies. In this composite material, shear deformation can occur since there is relative motion of the particles. A feature of early-age concrete is that the elastic region is much smaller than that of hardened concrete. Thus it may be reasonable to regard early-age concrete as a hardening visco-plastic material in which the saturation of pores with water decreases with age. However, a case where partial saturation with water is difficult if not impossible to understand theoretically. For simplicity, in this study, the pores are assumed to be saturated fully with pore water. The following formulation is based on this assumption.

2.1 CONSTITUTIVE LAW OF EARLY AGE CONCRETE

Here, concrete at an early age is modeled as a two-phase porous material composing aggregate and cement paste. A conceptual outline of the model is shown in Fig. 1. Aggregate particles are assumed to be elastic bodies, while cement paste is assumed to be a visco-plastic body. A stiffness matrix is formulated for the concrete such that the total concrete strain is a summation of individual weighted strains. When V_A denotes a volume of aggregate and V_C denotes a volume of cement paste, the total strain can be written as

$$d\{\varepsilon^T\} = \frac{V_A}{V} d\{\varepsilon_A^T\} + \frac{V_C}{V} d\{\varepsilon_C^T\}, V = V_A + V_C \quad (1)$$

where

$$d\{\varepsilon_A^T\} = d\{\varepsilon_A^e\} + d\{\varepsilon_A^{pr}\} + d\{\varepsilon_A^t\}$$

$$d\{\varepsilon_C^T\} = d\{\varepsilon_C^e\} + d\{\varepsilon_C^{pr}\} + d\{\varepsilon_C^t\} + d\{\varepsilon_C^{vp}\} + d\{\varepsilon_C^h\} \quad (2)$$

Here, the superscripts 'e', 'pr', 't', 'vp', and 'h' denote elasticity, pore pressure, temperature, visco-plasticity and contraction due to hydration, respectively. Subscript 'A' and 'C' denote aggregate and cement paste, respectively. The following relation between effective stress and total strain can be written:

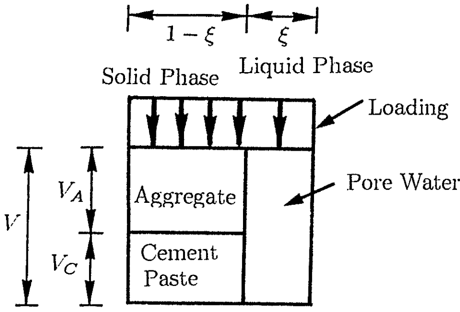

Fig.1 A Two Phase Porous Material Model

$$d\{\sigma'\} = (1-\xi)[D_A^e]d\{\varepsilon_A^e\} = (1-\xi)[D_C^e]d\{\varepsilon_C^e\} \quad (3)$$

where $[D_A^e]$ and $[D_C^e]$ are the elastic stiffness matrices of aggregate and cement paste respectively. ξ is porosity, which changes with both age and hydration. Substituting Eqns. (1) and (2) into Eqn. (3), the following equation can be obtained:

$$d\{\sigma'\} = (1-\xi)[D_S]\left(d\{\varepsilon^T\} - d\{\varepsilon^{pr}\} - d\{\varepsilon^t\} - \frac{V_C}{V} d\{\varepsilon^{vp}\} - \frac{V_C}{V} d\{\varepsilon^h\}\right) \quad (4)$$

where

$$d\{\varepsilon^T\} = \frac{V_A}{V} d\{\varepsilon_A^T\} + \frac{V_C}{V} d\{\varepsilon_C^T\} \quad (5)$$

$$d\{\varepsilon^t\} = \frac{V_A}{V} d\{\varepsilon_A^t\} + \frac{V_C}{V} d\{\varepsilon_C^t\} \quad (6)$$

$$d\{\varepsilon^{pr}\} = \frac{V_A}{V} d\{\varepsilon_A^{pr}\} + \frac{V_C}{V} d\{\varepsilon_C^{pr}\} \quad (7)$$

$$[D_S] = \left[\frac{V_A}{V}[D_A^e]^{-1} + \frac{V_C}{V}[D_C^e]^{-1}\right]^{-1} \quad (8)$$

Visco-plastic strain may be defined as follows.

$$d\{\varepsilon^{vp}\} = \Delta t \cdot \gamma \cdot F(\sigma')\left\{\frac{\partial F}{\partial \sigma'}\right\} \quad (9)$$

where F represents the surface of visco-plastic potential and extends or contracts with accumulated damage. γ is viscosity.

2.2 MODIFIED DRUCKER-PRAGER SURFACE AS VISCO-PLASTIC POTENTIAL

In this study, a Drucker Prager failure function is used to give the visco-plastic potential. It can be written as

$$F = \alpha I_1 + \sqrt{J_2} - k \tag{10}$$

in which I_1 and $\sqrt{J_2}$ denote the first invariant of the stress tensor and the second invariant of the deviatric stress tensor, respectively. α and k are material constants and change with both age and degree of hydration. In approximating the Mohr-Coulomb hexagonal surface by the Drucker-Prager cone, agreement is obtained along the compressive meridian where $\gamma_c = 60^\circ$. The two material constants then take the values

$$\alpha = \frac{2\sin\phi^*}{\sqrt{3}(3-\sin\phi^*)} \quad \text{and } k = \frac{6c^*\cos\phi^*}{\sqrt{3}(3-\sin\phi^*)} \tag{11}$$

where c^* and ϕ^* are mobilized cohesion and internal friction angle of the cement paste, respectively. c^* and ϕ^* can be defined as related to plastic strain history through a damage parameter, ω. Since, in general, ϕ^* is an increasing function of ω, while c^* is a decreasing function of ω,

$$c^* = c\exp[-(a\varpi)^2] \tag{12}$$

$$\phi^* = \begin{cases} \phi\sqrt{2\omega - \omega^2} & \omega \le 1 \\ \phi & \omega > 1 \end{cases} \tag{13}$$

where c and ϕ are the cohesion and internal friction of the cement paste, respectively, and change with age and hydration. a is material constant. As mentioned above, the failure surface is assumed to vary with the damage parameter in stress space. Using effective stress σ_e and effective plastic strain $d\varepsilon_p$, which are the values in the uniaxial state that is equivalent to the actual stress state, the incremental plastic work dW^p can be represented as

$$dW^p = \{\sigma'\}^T d\{\varepsilon^p\} = \sigma_e d\varepsilon_p \tag{14}$$

The damage parameter is defined as the degree of accumulated damage due to occurrence of micro crack [6], and can be expressed as

$$\omega = \frac{\beta}{\sigma_e \varepsilon_0}\int dW^p \tag{15}$$

where β is a material constant and

$$\varepsilon_0 = \frac{f_c'}{E_c} \tag{16}$$

where E_c and f_c' are the elastic modulus and uniaxial compressive strength of the cement paste, respectively. Substituting Eqn.(14) into Eqn.(15), the following equation is obtained

$$\omega = \beta\int \frac{1}{\varepsilon_0} d\varepsilon_p \tag{17}$$

2.3 ESTIMATION OF POROSITY BASED ON HYDRATION OF CEMENT PASTE

In the constitutive law described in Subsection (1), porosity is used to formulate the model and it is mentioned that porosity changes with age and hydration. Here, porosity will be estimated based on Kawasumi's study[7]. If hydration rate is assumed to be dependent on the free water content of the cement, hydration process can be expressed as follows.

$$\frac{dC_H}{dt} = k_0(1-n_0)t^{-n_0}(W-\gamma_p C_H)(C-C_H) \tag{18}$$

where C, C_H and W are the initial cement content, the hydrated cement content and the initial water content per cubic meter and $\gamma_p C_H$ is the hydrated water content. γ_p is the water-cement ratio of completely hydrated, and takes value of 0.25~0.38. The age, t, has a unit of days. k_0 and n_0 are hydration parameters and, under water curing at a temperature of 20 ℃, takes values of 7.419×10^{-1} and 8.928×10^{-6}, respectively. Solving Eqn.(18) under the initial condition of $C_H = 0$ at $t = 0$, then

$$C_H = \frac{1-\exp\left[(\gamma_p C - W)k_0 t^{1-n_0}\right]}{1-\gamma_p C/W \exp\left[(\gamma_p C - W)k_0 t^{1-n_0}\right]}\times C \qquad \text{for } \frac{W}{C}\neq\gamma_p \tag{19}$$

$$C_H = \frac{\gamma_p k_0 t^{1-n_0}}{1+\gamma_p k_0 t^{1-n_0}}\times C \qquad \text{for } \frac{W}{C}=\gamma_p \tag{20}$$

Considering the reduction of pore water due to hydration from the initial water content V_{W0}, the porosity ξ can be represented as

$$\xi = V_{W0}(1-\gamma_p C_H/W) \tag{21}$$

2.4 FORCE EQUILIBRIUM EQUATION BY PRINCIPLE OF VIRTUAL WORK

If pore water pressure p exists, the relation between total stress $\{\sigma\}$ and effective stress $\{\sigma'\}$ can be written as

$$\{\sigma\} = \{\sigma'\} - \{m\}p \tag{22}$$

$$\{m\} = \{1 \quad 1 \quad 1 \quad 0 \quad 0 \quad 0\}^T \tag{23}$$

where tension is taken as a positive stress, while compression is taken as a positive pore water pressure. Using principle of virtual work, the equilibrium condition can be expressed as

$$\int_\Omega \delta\{\varepsilon\}^T\{\sigma\}d\Omega - \int_\Omega \delta\{u\}^T\{b\}d\Omega - \int_\gamma \delta\{u\}^T\{t\}d\gamma = 0 \tag{24}$$

where $\{b\}$ and $\{t\}$ are body force and surface traction and Ω and γ denote the domain and surface boundaries, respectively. Using a suitable shape function, Eqn.(24) can be rewritten in matrix form as

$$K_T\frac{d\{\bar{u}\}}{dt} - L\frac{d\{\bar{p}\}}{dt} - A\frac{d\{\bar{T}\}}{dt} - \frac{d\{\bar{f}\}}{dt} = 0 \tag{25}$$

where matrices K_T, L and A are the tangential stiffness matrix, a matrix representing the effect of pore water pressure and compressibility of solid and liquid, and the matrix of the effect of temperature, respectively. $\{\bar{f}\}$ denotes an external force vector. These matrices and vector can be expressed as

$$K_T = \int_\Omega (1-\xi) B^T D_S B d\Omega \tag{26}$$

$$L = \int_\Omega \xi B^T \{m\} \bar{N} d\Omega \tag{27}$$

$$A = \int_\Omega (1-\xi) B^T D_S \{m\} \alpha \bar{N} d\Omega \tag{28}$$

$$\{\bar{f}\} = \int_\Omega N^T \{b\} d\Omega + \int_\gamma N^T \{t\} d\gamma \tag{29}$$

where N, $\bar{N}$, and B are shape function matrices with respect to displacement, pore water pressure and temperature, and strain and displacement, respectively. If solid particles are assumed to be non-compressible under pore water pressure, as in soil mechanics, both $(1-\xi)$ and ξ can be replaced by unity.

2.5 MASS CONSERVATION LAW OF PORE WATER

If the velocity of water migration is assumed to be governed by the gradient of Gibb's free energy, G, per unit mass [4]), then

$$\{v\} = -k\nabla G \tag{30}$$

where k is permeability. G can be expressed for the different phases as follows.

$$\begin{aligned} &\text{liquid phase} \quad && G = (\gamma_w z + p)/\gamma_w + G_{sat} \\ &\text{gas phase} \quad && G = (R/M)T \ln H + G_{sat} \end{aligned} \tag{31}$$

where γ_w and z denote the unit weight of water and the vertical coordinate, respectively, and R, H, and M are the gas constant, p/p_{sat} (p_{sat} is the critical saturated vapor pressure), and the molecular weight of water, respectively. Moreover, G_{sat} is the standard free energy and is a function of only absolute temperature. In this study, voids are assumed to be perfectly saturated by the liquid phase, and moreover the absolute temperature is assumed to be constant. Consequently,

$$\{v\} = -k\nabla \frac{\gamma_w z + p}{\gamma_w} \tag{32}$$

the mass conservation law indicates that the accumulated amount of fluid is equivalent to the difference between inflow and outflow. This accumulation may include the following factors:

1) A change in total strain

$$\frac{d\varepsilon_v}{dt} = \{m\}^T \frac{d\{\varepsilon\}}{dt}$$

2) A change in the particle volume due to pore water pressure

$$(1-\xi)\{m\}^T D_S{}^{-1}\{m\}\frac{dp}{dt}$$

3) A change in the volume of fluid

$$\frac{\xi}{k_f}\frac{dp}{dt}$$

4) A change in fluid volume due to temperature

$$-3\xi\mu\frac{dT}{dt}$$

5) A change in the particle volume due to the change in effective stress

$$-\{m\}^T D_S{}^{-1}\frac{d\{\sigma'\}}{dt}$$

Here, k_f and μ are the bulk modulus of water and the thermal expansion coefficient of water, respectively. If the total accumulation in a control volume is the summation of the terms 1) to 5) above, the mass conservation law can be finally expressed as

$$\xi\{m\}^T\frac{d\{\varepsilon\}}{dt}+\frac{\xi}{k_f}\frac{dp}{dt}+3\xi\mu\frac{dT}{dt}-\nabla^T k/\gamma_w\nabla(\gamma_w z+p)-q=0 \qquad (33)$$

where q is the inflow of pore water. Using the Galarkin method, Eqn.(33) can be reduced into the discrete form

$$-H\{\bar{p}\}-L^T\frac{d\{\bar{u}\}}{dt}-S\frac{d\{\bar{p}\}}{dt}-W\frac{d\{\bar{T}\}}{dt}+\{f_p\}=0 \qquad (34)$$

where

$$H=\int_\Omega(\nabla\bar{N})^T k/\gamma_w\nabla\bar{N}d\Omega\ ,\quad S=\int_\Omega\bar{N}^T\frac{\xi}{k_f}\bar{N}d\Omega\ ,\quad W=\int_\Omega\bar{N}^T\{3(1-\xi)\alpha-3\xi\mu\}\bar{N}d\Omega$$

$$\{f_p\}=\int_\Omega\bar{N}^T q d\Omega-\int_\Omega(\nabla\bar{N})^T k/\gamma_w\nabla\gamma_w z d\Omega+\int_\gamma\bar{N}^T(\{v\}^T\cdot n)d\gamma$$

If non-compressibility is assumed, one can set $k_f=\infty$ and $\xi=1$ in this equation.

2.6 GOVERNING EQUATIONS FOR TWO-PHASE POROUS MATERIAL

Finally, from Eqns. (25) and (34), a coupling equation for the force equilibrium condition and mass conservation of pore water can be expressed in matrix form as

$$\begin{bmatrix} 0 & 0 \\ 0 & -H \end{bmatrix} \begin{Bmatrix} \{\bar{u}\} \\ \{\bar{p}\} \end{Bmatrix} + \begin{bmatrix} K_T & -L \\ -L & -S \end{bmatrix} \begin{Bmatrix} \dfrac{d\{\bar{u}\}}{dt} \\ \dfrac{d\{\bar{p}\}}{dt} \end{Bmatrix} = \begin{Bmatrix} \dfrac{d\{\bar{f}\}}{dt} + A\dfrac{d\{\bar{T}\}}{dt} \\ W\dfrac{d\{\bar{T}\}}{dt} - f_p \end{Bmatrix} \tag{35}$$

Since the symmetry of all the matrices in this equation is guaranteed, one can obtain solution if both the initial and boundary conditions are known in advance. Expressing Eqns. (35) using the reverse finite difference method, the following equation can be obtained:

$$\begin{bmatrix} K_T & -L \\ -L & -S - H\Delta t_n \end{bmatrix} \begin{Bmatrix} \Delta\bar{u}_n \\ \Delta\bar{p}_n \end{Bmatrix} = \begin{Bmatrix} \Delta\bar{f}_n + A\Delta\bar{T}_n \\ -f_{pn}\Delta t_n + W\Delta\bar{T}_n + H\bar{p}_{n-1}\Delta t_n \end{Bmatrix} \tag{36}$$

where

$$\Delta\bar{u}_n = \bar{u}_n - \bar{u}_{n-1}, \quad \Delta\bar{p}_n = \bar{p}_n - \bar{p}_{n-1}, \quad \Delta\bar{T}_n = \bar{T}_n - \bar{T}_{n-1},$$
$$\Delta\bar{f}_n = \bar{f}_n - \bar{f}_{n-1}, \quad t_{n-1} + \Delta t_n = t_n \tag{37}$$

Basically, this formulation is similar to expressing only one element in the generalized Maxwell model. Individual viscosity is defined as the dashpot parallel for the plastic component. By increasing the number of elements and introducing a failure surface, it will be extended to the general creep problem

3. ESTIMATION OF MATERIAL PARAMETERS

3.1 COHESION AND INTERNAL FRICTION ANGLE OF EARLY-AGE CONCRETE

In a modified Drucker-Plager material, it is necessary to determine several parameters including cohesion, internal friction angle, and the damage parameters such as α, and β. The relation between cohesion and internal friction angle cannot be determined by uniaxial compressive tests on early age concrete. To investigate this relation, triaxial tests using a specimens with a size of 5cm×10cm were performed at ages of 12, 24, 36, and 48 hours. The water cement ratio was 55% and the specimens were cured in the atmosphere at a temperature of 25℃. The resulting relation between cohesion in early-age cement paste and maturity is shown in Fig.2. Cohesion clearly increases with maturity, but, little cohesion occurs until 12 hours. Since the specimens were casted at 25℃, larger value of cohesion would be obtained if the temperature were higher. Maturity is defined as the multiplier of a function of environmental temperature and a age at that temperature, and can be expressed as

$$t_e = \int_0^t \exp\left[\frac{U_h}{R}\left(\frac{1}{293} - \frac{1}{K}\right)\right] dt \tag{38}$$

where K is absolute temperature (K), U_h is the activation energy of hydration (J/mol), and R is the gas constant (J/mol K). The relation between internal friction angle and maturity is shown in Fig.3. The internal friction angle does not vary much with maturity and ranges in value from 25 to 35° . However, the applicability of these parameters to general mixtures cannot be investigated using only these results. The same is true in the case of cohesion. In the analysis performed in the next section, the internal friction angle is assumed to be a constant value of 27° , the mean of the experimental data, because It is regarded as invariant with maturity. Although cohesion is regarded as almost one-third value of uniaxial strength, creep flow may occur in early-age concrete, which is a visco-plastic body, even with relatively tiny stress levels. Consequently, the cohesion of visco-plastic potential is assumed to be one-third value of ordinary cohesion i.e. one-ninth the value of uniaxial strength, although this is a very rough assumption.

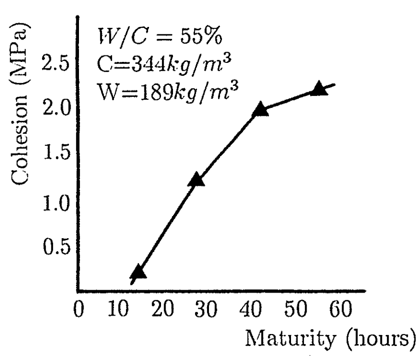

Fig.2 Cohesion with Maturity

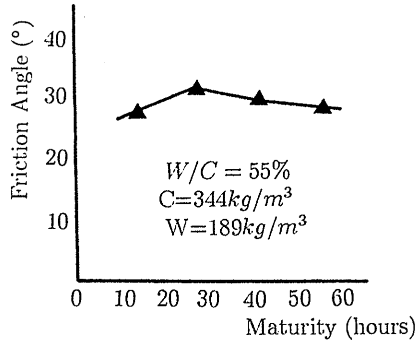

Fig.3 Friction Angle with Maturity

3.2 POROSITY AND PERMEABILITY

The initial porosity can be obtained from the mix proportion on the assumption that it is equivalent to the volumetric ratio of water to total volume. Porosity decreases as chemical hydration advances with age. Thus porosity can be calculated from the reduction in initial water volume. With respect to permeability, the principle proposed Darcy and Poiseuille may be applicable. However, this is not guaranteed because there is no experimental evidence with respect to permeability. In this study, the value of the permeability used is estimated roughly from past studies of permeability. Murata[8] carried out permeability tests on hardened concrete at 28 days and estimated the relation between permeability and water-cement ratio. The results of these tests are shown in Fig. 4. He also reported that permeability at 28 days was 0.6 times that at 14 days; however, he did not report in detail on the permeability before 14 days. Permeability before 14 days can be extrapolated considering T.C. Powers's study[3], in which he reported that the permeability of hardened concrete was 1.0^{-6} times the initial value. His experimental results are shown in Fig.5. It is found that the permeability at 5 days is 10^{-4} times the initial value and, moreover, at 14 days is 10^{-2} times the value at 5 days. The results given in Fig. 5 are for cement paste; the reduction in permeability of concrete with age has atill not been clarified experimentally. In this study, the reduction rates given in Fig. 5 for cement paste are assumed to apply directly to the whole concrete. Values such as internal friction angle, cohesion, and permeability should, of course, be investigated further.

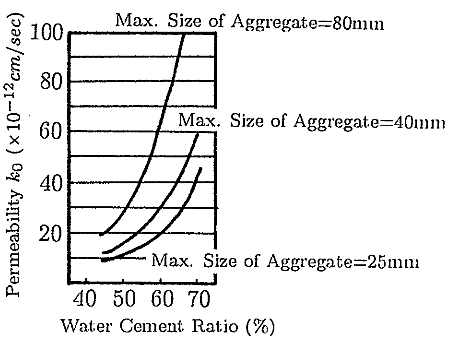

Fig.4 Experimental Permeability (Murata)

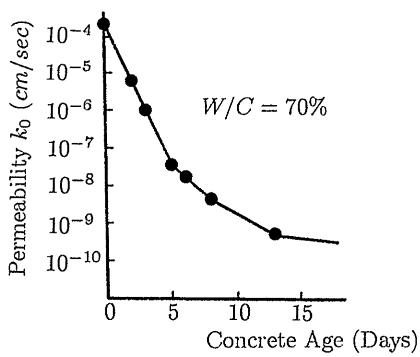

Fig.5 Experimental Permeability of Cement Paste(Powers)

4. ANALYSIS OF EARLY-AGE CONCRETE

Using the model constructed in Section 2, the experimental results reported by certain researchers are analyzed. One of the most important features of the model is that pore water pressure as well as effective stress can be calculated explicitly.

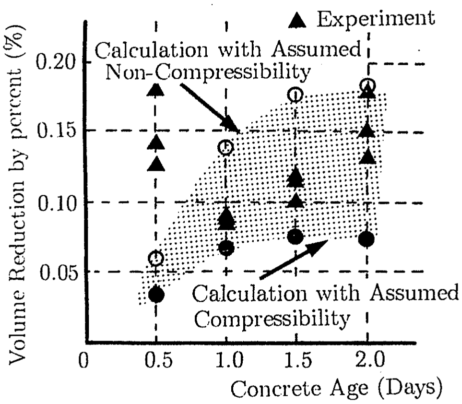

Fig.6 Drain out of pore Water

4.1 ANALYSIS OF PORE WATER DRAINAGE TEST

The first analysis is of pore water drainage in early-age mortar[9]. Mortar specimens were made with a size of 5cm×10cm. The mix proportion was W/C=63% with unit cement and sand contents are 368kg/m^3 of 1175kg/m^3, respectively. The specimens were cured under water in a temperature bath of 20±3℃ until testing. The specimens were taken from the water and wiped quickly with a dry cloth before their mass was measured with an electronic instrument able to measure to 0.01 accuracy. Next, uniaxial compressive loading was applied to the specimen at a constant displacement rate (1.0×10^{-3}cm/s) until loading stress reached the peak state. After loading, the specimen was wiped quickly and its mass is measured again. The results are shown in Fig.6, which is the relation between concrete age and volume reduction. This indicates that pore water drains out at every age and the value is in the range of 0.1 ~ 0.2%. The experimental results for every age have a relatively small error compared to mean value , so it can be assumed that errors due to wiping are small. The mass of specimens of course decreases with evaporation, so the weight loss due to evaporation was also measured during loading. Results indicate that the weight loss due to evaporation is very small compared with that due to loading. Consequently, the experimental results obtained can be regarded as the drainage of pore water due to loading.

To analyze the experimental results, it is necessary to know the time variation of certain material parameters, such as cohesion and internal friction angle. Elastic modulus is extrapolated from experimental data of elastic modulus at 24 days, although this is a very rough assumption, giving values at 0.5, 1.0, 1.5 and 2.0 days of 250, 500, 750 and, 1000 Mpa, respectively. Cohesion is estimated as $c = f'_c/2$ from Mohr's circle

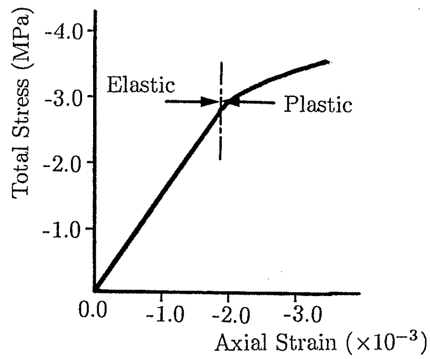

(a) Total Stress

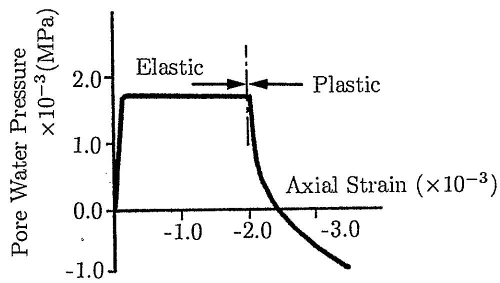

(b) Pore Pressure

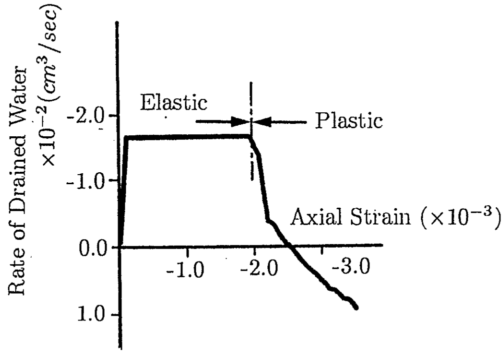

(c) Rate of Drainage

Fig.7 Axial-Atrain-Pore Pressure-Drained out Water

and internal friction angle is assumed to be constant at 27° .
Porosity and permeability are estimated from Eqn.(21) and Section 3. On the surface boundary condition with respect to pore water, the pore water pressure is regarded as equivalent to atmospheric pressure. Analytical results for volume reduction, rate of drainage, pore water pressure, and total stress are shown in Fig.6 and Fig.7. Figure 7 indicates both experimental and analytical results. Drainage is rapid as soon as the load is applied and remains constant. However, once the elastic limit is exceeded, the drainage rate becomes negative: i.e. suction occurs because of dilation due to plastic volumetric strain. In the analysis, since inflow from the outside is not considered, the total drainage of pore water is calculated from the product of time and drainage rate until the elastic limit. The experimental results in Fig.6, except that at 0.5 days lie between two analytical curves. one obtained taking the compressibility of both water and cement paste into account, and the other assuming non-compressibility as is often the case in soil mechanics. The experimental and analytical values are of the same order despite the very rough of material parameters. The experimental results are not systematic with age, while the analytical curves do systematically increase.

4.2 ANALYSIS OF CREEP

Creep analysis is carried out with the proposed model using experimental results on early-age concrete performed by the Central Research Institute of the Electric Power Industry (CRIEPI)[10]. The mix proportion used in these experiments was such that W/C=49% and the unit cement, water, fine aggregate, and gravel aggregate contents were 339, 166, 730, and 1063 kg/m^3, respectively. The specimens were cylindrical, with a size of ϕ =15cm × 30cm. They were removed from the mold after 5 hours. The specimens were placed in copper cans and the lids were welded immediately after insertion. At the ages of 0.69 days, 1.0 day, and 3.0 days, loads were applied to reach the stress levels of 1.0, 2.0 and 2.5 Mpa. The stress level ratios for the uniaxial strength are 45%, 38% and 22%, respectively. The experimental results of the creep tests are shown in Fig.8. The most significant feature is that in every case, creep strain rises instantaneously just after loading and remains constant for some time before beginning to increase gradually again. In analyzing these results, each elastic modulus is adopted to coincide the experimental initial strain with calculated initial strain. Initial cohesion and internal friction angle are given as the method by Section 3.1 and Section 3.2. The viscosity coefficient is given in decreasing form with age, ranging from 5.0×10^{-5} to 3.0×10^{-5} /Mpa/Day since the visco-plastic component may have less effect an deformation with age. The analysis is carried out with the same stress level as the experiments. The results calculated by the model are shown in Fig.8. It should be noted that the calculated results do not take into account the compressibility of both solid and liquid phases. The creep calculated strain rises instantaneously within for a few hours of loading and then increases gradually. In other words, the pore water pressure immediately after loading is translated rapidly into effective stress, and creep strain rises rapidly because of the drainage of pore water. Creep strain

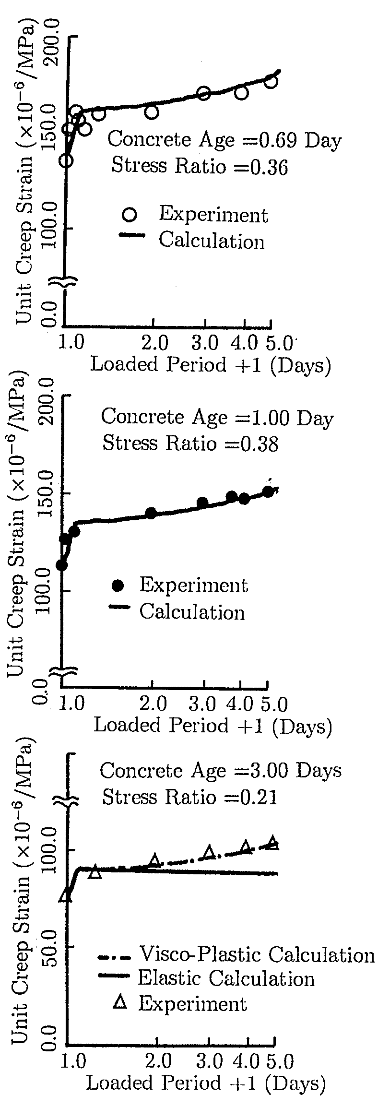

Fig.8 Compressive Creep Strain in Early-Age Concrete

ceases when pore water stops migrating. Thereafter, creep strain increases gradually due to visco-plastic deformation. The major feature of the proposed visco-plastic deformation analysis method is the considerable dependence of visco-plastic surface and viscosity coefficient. It is clear that further study of the visco-plastic surface and viscosity coefficient is needed. Although, this analysis takes into account the compressibility of solid and liquid, the results give no creep strain, which indicates that if the rapid increase of creep strain is explained by the migration of pore water, the assumption of the compressibility is less valid than the other assumption in the creep analysis.

4.3 ANALYSIS OF RELAXATION

The proposed model is used to carry out relaxation analysis of results obtained in experiments performed at Gifu University[11]. These tests were carried out for both compressive and tensile relaxation. In the tensile relaxation tests, specimens 10cm×10cm×86cm were used, while in the compressive relaxation tests, they were 10cm×10cm×40cm. The mix proportion was such that W/C=50%, s/a=44%, and unit cement, water, fine aggregate, and gravel aggregate contents were 346, 173, 790, and 996 kg/m^3, respectively. The specimens were cured in a steam room at 20℃ and R.H=90% and both compressive and tensile relaxation tests were carried out at the age of 1, 3, 7, and 28 days. The stress levels in the tensile relaxation tests were 30%, 30%~50%, and over 60% for tensile strength, while in the compressive relaxation tests, they were 30%, 50%, and 80% for compressive strength. The specimens were removed from the humid atmosphere and sealed with the paraffin to prevent loss of water. The specimens were also kept at a constant 20℃ during the test. The results obtained in the test are shown in Fig 9 to 11.

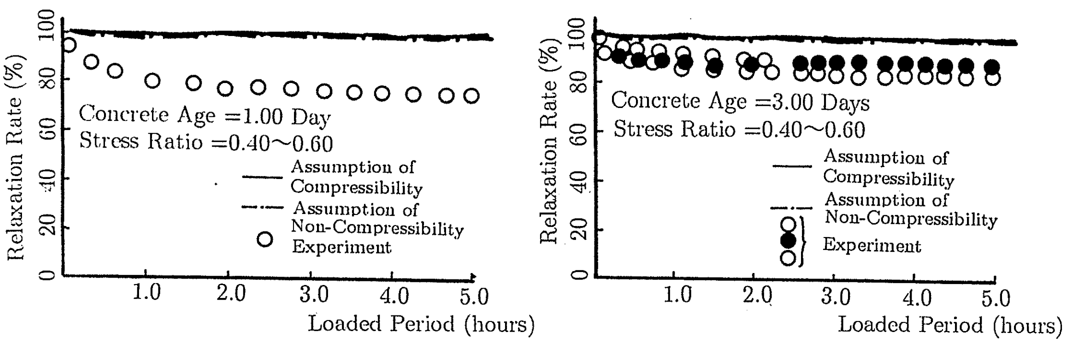

Fig.9 Tensile Relaxation of Early-Age Concrete

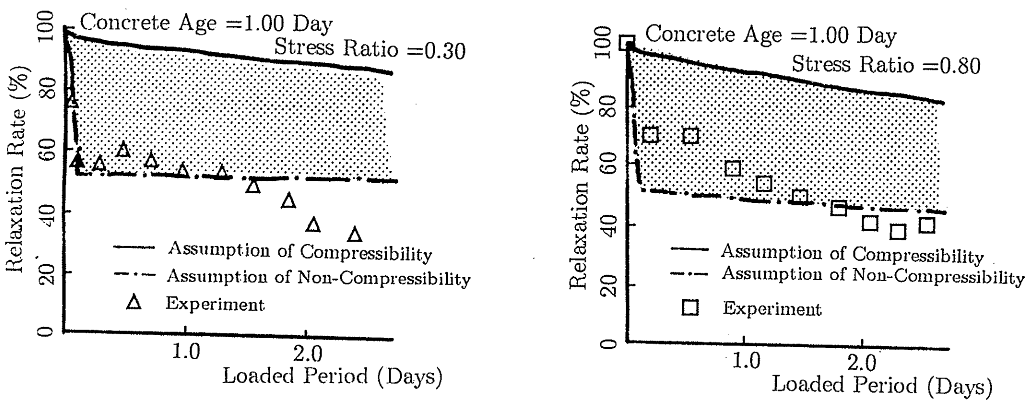

Fig.10 Compressive Relaxation of Early-Age Concrete(Age=1.0Day)

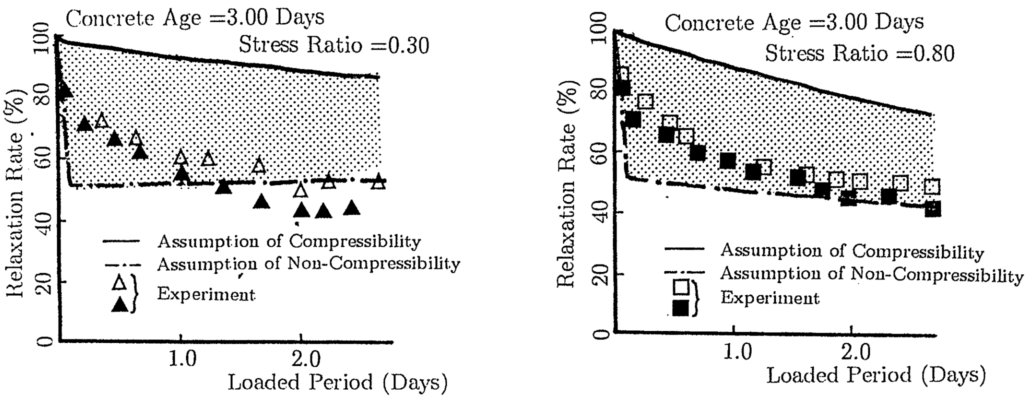

Fig. 11 Compressive Relaxation of Early-Age Concrete(Age=3.0Day)

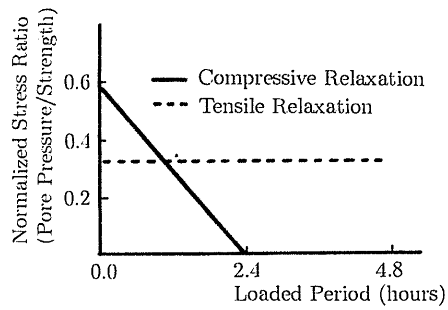

Fig. 12 Variation of Pressure in the Relaxation

It is found that the stress relaxation in the tensile relaxation test is less than that in the compressive relaxation test. Analysis was carried out for these experimental results. As a boundary condition, the pore water pressure at the surface was made equivalent to atmosphere in the compressive relaxation case. In other words, in the compressive relaxation analysis, pore water is allowed to move from the surface. In the experiment, the specimens had a paraffin coating, so this assumption implies that the paraffin was insufficient to prevent the outflow of pore water from the concrete. However, since a paraffin coating can prevent the inflow of water, pore water is assumed to not flow across the surface during tensile relaxation. The permeability is given as mentioned in the Sec.3.2. The viscosity coefficient value is the same as previously used in the creep analysis. The calculated results are also shown in Figs.9 to 11. In the compressive relaxation analysis, the stress relaxes rapidly within a few hours in comparison to initial stress level, which indicates that pore water plays an important role in compressive relaxation. The experimental results lie between two analytical curves, one where compressibility is assumed for both solid and liquid, and the other where they were assumed non-compressible. The actual mechanism of relaxation thus should exist between the two curves. While in tensile relaxation, the stress relaxes very little in all cases. This is clear from the figure because there is no effect of water migration in the tensile relaxation analysis. The experimental results are basically the same as the calculated ones, although the experimental values are a little larger. This analysis of relaxation gives less satisfactory results than the creep analysis. In other words, a different mechanism of deformation acts in creep and relaxation simulations. Figure 12 shows the variation in normalized pore water pressure with age. The deviation in tensile and compressive relaxation in the analysis depends on whether migration of pore water is assumed to exist or not.

4.4 ANALYSIS OF TRIAXIAL COMPRESSIVE TEST

Replacing the visco-plastic potential by a plastic potential, the proposed model can be used to capture stress and strain relations in the elasto-plastic system. As an example, analysis is carried out using the model in which plastic potential is used for triaxial compressive tests[9]. The specimens, with mixture and size specification identical to those in Sec.4.1, were subjected to triaxial tests at the age of 22, 24, and 26 hours. The lateral pressure was held constant at 0.5 Mpa during the tests. Figures 13 to 15 show the experimental and analytical relations between axial strain and $\sqrt{J_2}$, as well as analytical results of pore water pressure changes accompanying strain change. Generally, if a lateral pressure of less than one third value of the uniaxial compressive strength is applied, concrete collapses in a brittle manner and reveals strain softening behaviour. The uniaxial strength at the age of 22~26 hours is a value in the range 1.8~3.0Mpa. Thus the lateral pressure is clearly less than one third, yet, in every experimental case, there was no brittle collapse behaviour. Analytically, pore water pressure increases with increasing axial strain until the elastic limit. However, beyond the elastic limit, pore water pressure decreases with increasing axial strain because plastic volumetric dilation occurs. At the same time, the effective stress component increases with decreasing the pore water pressure. Thus there is a case where concrete reveals no strain softening if the magnitude of the pore water pressure is above a certain value. Consequently, if concrete collapse is induced as a result of effective stress, concrete collapse is affected strongly by the pore water pressure because concrete has poor permeability.

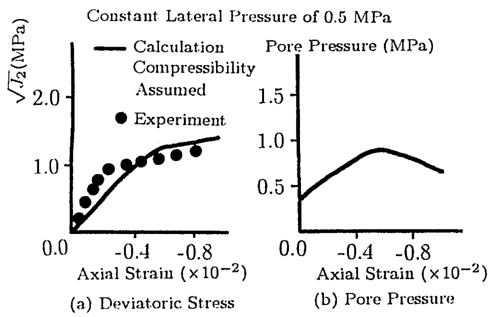

Fig.13 Three Axial Test of Early-Age Concrete (Age=22hrs.)

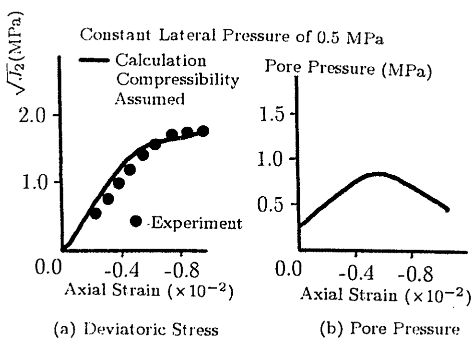

Fig.14 Three Axial Test of Early-Age Concrete (Age=24hrs.)

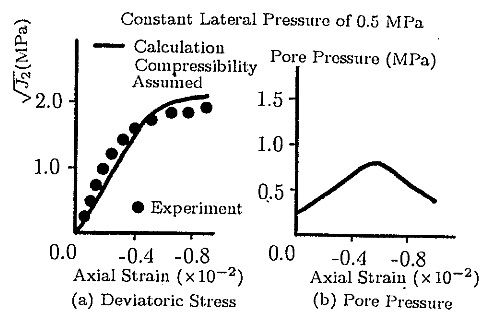

Fig.15 Three Axial Test of Early-Age Concrete (Age=26hrs.)

5. CONCLUSION

In this paper, the time-dependent behaviour of early-age concrete is discussed from the viewpoint of pore water. First of all, a mathematical model that takes into account the compressibility of both solid and liquid is introduced. Then analysis is carried out using the proposed model to compute creep and relaxation as well as drainage of pore water with experimental results. Behaviour is discussed analytically in terms of pore water.

The conclusions reached can be summarized as follows.

(1) Tests on pore water drainage confirm that outflows of pore water occur.

(2) Analysis of creep tests and relaxation tests demonstrate the relevancy of the proposed model, although material parameters such as cohesion, permeability, and viscosity coefficient are not rigorously discussed.

(3) Pore water or pore water pressure may strongly affect the behaviour of early-age concrete.

REFERENCES

1) Iwasaki, N.: Properties of Concrete, Kyouritsu Pub. Cop. pp.55-58, Sep. 1975
2) Lynam, C. G.: Growth and Movement in Portland Cement Paste Concrete, London, Oxford Univ. Press, pp.139, 1934
3) Powers, P. C., Copeland, L. E., Hayes, J. C. and Mann, H. M.: Permeability of Portland Cement Paste, ACI Journal, No.51-14, pp.285-298, Nov., 1954
4) Bazant, Z. P., and Najjar, L.: Nonlinear Water Diffusion in Nonsaturated Concrete, Materiaux et Constructions, Vol.5, No.25, pp.3-20, 1972
5) Neville, A. M.: Current Problems Regarding Concrete under sustained Loading, Intern. Ass. For Bridge and Structural Engineering, 26, pp.337-343, 1966
6) Wu, Z. S., and Tanabe, T.: A Hardening-softening Model of Concrete Subjected to Compressive Loading, Journal of Structural Engineering, Architectual Institute of Japan, Vol.36B, pp.153-162, 1990
7) Kawasumi, M., Kasahara, K., and Kuriyama, T.: Creep of Concrete at Elevated Temperatures, CRIEP Report, No.380037, pp.15-16, Feb., 1981
8) Murata, J.: Studies on the Permeability of Concrete, Trans. Of JSCE, No.77, pp.69-103, Nov., 1961
9) Ishikawa, Y., Ohshita, H., and Tanabe T.: The Thermal Stress Analysis of Early Age Massive Concrete with Concrete Model as Saturated Permeable Material, Trans. of the Japan Concrete Institute, Vol.15, pp.123-130, 1993
10) Haraguchi, A., Kawasumi, M., Tanabe, T., and Okazawa, T.: Study on Concreting Schedule of Kuroda Dam, Part 1 (Mechanical and Thermal Properties of Concrete), CRIEP Report, No.375561,pp.2-36, July, 1976
11) Morimoto, H., Hirata, M., and Koyanagi, W.: On the Stress Relaxation of Concrete at an Early Age and Its Estimation Method, Proc. of JSCE, N0.396, V-6, pp.59-68, August, 1988